6-1-2016

Defect Driven Magnetism in Doped SnO_2 Nanoparticles: Surface Effects

Pushpa Raghani
Boise State University

Pankaj Kumar
Boise State University

Balaji Ramanujam
Boise State University

Alex Punnoose
Boise State University

Publication Information

Raghani, Pushpa; Pankaj, Kumar; Balaji, Ramanujam; and Punnoose, Alex. (2016). "Defect Driven Magnetism in Doped SnO_2 Nanoparticles: Surface Effects". *Journal of Magnetism and Magnetic Materials, 407*, 46-50. doi: 10.1016/j.jmmm.2016.01.050

Defect driven magnetism in doped SnO_2 nanoparticles: Surface effects

Raghani Pushpa, Pankaj Kumar, Balaji Ramanujam and Alex Punnoose

Department of Physics, Boise State University

Boise, ID, USA

Email: pankajsahota@gmail.com

Magnetism and energetics of intrinsic and extrinsic defects and defect clusters in bulk and surfaces of SnO_2 is investigated using first-principles to understand the role of surfaces in inducing magnetism in Zn doped nanoparticles. We find that Sn vacancies induce the largest magnetic moment in bulk and on surfaces. However, they have very large formation energies in bulk as well as on surfaces. Oxygen vacancies on the other hand are much easier to create than V_{Sn}, but neutral and V_O^{+2} vacancies do not induce any magnetism in bulk as well as on surfaces. V_O^{+1} induce small magnetism in bulk and on (001) surfaces. Isolated Zn_{Sn} defects are found to be much easier to create than isolated Sn vacancies and induce magnetism in bulk as well on surfaces. Due to charge compensation, $Zn_{Sn}+V_O$ defect cluster is found to have the lowest formation energy amongst all the defects; it has a large magnetic moment on (001), a small magnetic moment on (110) surface and it is non-magnetic in bulk. Thus, we find that Zn_{Sn} and $Zn_{Sn}+V_O$ defects on the surfaces of SnO_2 play an important role in inducing the magnetism in Zn-doped SnO_2 nanoparticles.

Keywords—density functional theory; defects; defect formation energies; magnetism

1. INTRODUCTION

Recently, ferromagnetism in dilute magnetic semiconductors (DMS) has received a considerable attention owing to potential applications in spintronic and optoelectronic devices [1, 2]. In DMS, magnetism can be induced in many ways. For instance, doping with magnetic transition metal (TM) is a one of the well-accepted ways of inducing magnetism in DMS. However, doping with magnetic TMs can lead to segregation and precipitation, which can limit the applications of these compounds [4-9]. Therefore, an extensive research is undergoing to overcome these difficulties. The oxide based DMS are an ideal choice for induced magnetism in the presence of defects, as these systems have high Curie temperature (T_C). It has been found experimentally that some of the semiconductor oxides and nitrides show induced magnetism with nonmagnetic dopants such as Li, C, N, Zn and Cd. Examples include wide band gap semiconductors such as ZnO [10-12], TiO_2 [13] and SnO_2 [14-20].

Among the oxide semiconductors, SnO_2 has drawn much interest due to the fascinating properties such as wide band gap, high optical transparency, electrical conductivity and chemical sensitivity [21-23]. These properties make SnO_2 based structures an ideal candidate for many applications such as in solar cells and catalysis [24]. Recent reports on doping the bulk and nanoparticles of SnO_2 with magnetic TMs have shown huge ferromagnetism at room and above room temperatures. The possibility of room and high temperature ferromagnetism in magnetic TM doped SnO_2 systems has got a lot of attention in the field of DMS due to its applications in spintronic devices [25-33]. However, the exact mechanism of induced magnetism in the nanoparticles of SnO_2 with nonmagnetic dopants is still under debate. Nonmagnetic TM atom (Zn, Cu) doped nanoparticles of SnO_2 give rise to a large magnetic moment as compared to their bulk counterparts. To understand the onset of this magnetism, we study the intrinsic and extrinsic defects and defect clusters on various surfaces of SnO_2 in a nanoparticle [34-38].

A nanoparticle of a material can have a number of orientations of the surfaces. The areal predominance of these surfaces will depend upon the surface energy — energy per unit area of the surface, *i.e.*, the surface with highest energy will have lowest area and vice-versa. However, the exact ratio of the different surfaces in a nanoparticle will depend upon the experimental conditions such as temperature and pressure. Due to anisotropic nature of surfaces, they will exhibit anisotropic magnetic properties, e.g., magnetism and magnetic anisotropy can be altered by

changing the chemical composition by creating the defects [39-41]. The overall magnetization of a nanoparticle will be a complex interplay among the magnetizations induced on different surfaces. To predict the overall magnetization of a nanoparticle, a much more complex modeling is required which is beyond the scope of this paper. In principle, one needs to calculate the formation energy (FE), magnetism and easy axis of magnetization for all the surfaces that would exist in a nanoparticle, which is a formidable task. Instead, we investigate the magnetism and energetics of two surfaces having the highest and the lowest surface energies of 11.23 and 6.23 eV/Å^2 (1.82 and 1.01 J/m^2) for (001) and (110) respectively, which are comparable to the values found in literature [36, 42, 43]. Using density functional theory (DFT), we study the effect of intrinsic defects and defect clusters such as V_O, V_{Sn}, Zn_{Sn}+V_O and Zn_{Sn}+V_{Sn} on the electronic and magnetic properties of bulk and (001) and (110) surfaces of SnO_2. We find that Zn_{Sn}+V_O defect clusters have the lowest FE of all the defects considered in this paper and the FE further decreases on the surfaces and is minimum on (110) surface. The Zn_{Sn}+V_{Sn} defect on the other hand leads to a huge magnetic moment on (110) surface but it has higher FE as compared to the Zn_{Sn}+V_O defect. By calculating the magnetic moments of Sn vacancies on symmetric (S) and asymmetric (A) (001) and (110) surfaces of SnO_2, we find that easy axis of magnetization for V_{Sn} on (001) is out of plane whereas it is in-plane for (110).

2. COMPUTATIONAL DETAILS

We use DFT to study the electronic and magnetic properties of various point defects and defect clusters in bulk SnO_2 and its (001) & (110) surfaces. Surfaces are modeled using slabs of atomic layers separated by a vacuum. Within DFT, we employ the pseudopotential formalism as implemented in Quantum-ESPRESSO [44]. Interactions between the valence electrons and nuclei are treated using norm-conserving scalar relativistic pseudopotentials. The generalized gradient approximation (GGA) is employed for the exchange-correlation potential with Perdew-Burke-Ernzerhof (PBE) exchange correlation functional [45]. The pseudopotentials of Sn, O and Zn are generated from their atomic configurations [Kr] $4d^{10}$ $5s^2$ $5p^2$, $1s^2$ $2s^2$ $2p^4$ and [Ar] $3d^{10}$ $4s^2$. The corresponding valency of the atoms is +4,-2 and +2, respectively. In general, SnO_2 crystallizes in the rutile structure. The optimized lattice parameters are $a = b = 4.843$ Å and $c = 3.314$ Å which are comparable to the earlier experimental and theoretical findings [5, 46]. To do the electronic

structure calculations, we use a Monkhorst-Pack scheme to generate the *k*-points [47]. For the 1×1×1 unit cell that contains two Sn and four O atoms, a *k*-mesh of 6×6×9 is used. For larger supercells, the *k*-mesh size is changed proportionally. A plane wave kinetic energy cutoff of 100 Ry is used for all calculations and forces are converged to 0.01 eV/Å.

To determine the direction of magnetization axis, we use symmetric and asymmetric slabs. If the magnetization is perpendicular to the surface, then the total magnetization of the symmetric slab will be zero whereas it will be non-zero for an asymmetric slab. We realize that this is a crude way of determining the direction of magnetization axis and one has to perform anisotropy calculations including spin-orbit coupling. However, these calculations can be computationally demanding and time-consuming especially for large supercells used in this work. The symmetric slab contains seven atomic layers. The central three layers are fixed at their bulk-like sites, and rest of the layers on top and bottom of the slabs are allowed to relax. The in-plane size of the supercell is 2×2×3 along both (001) and (110) directions with a vacuum of ~13 Å along the z-direction. The asymmetric slab contains five atomic layers, having bottom three layers fixed at bulk-like sites. The schematic picture of a (110)-oriented slab with Zn_{Sn}+V_{Sn} defect is shown in fig.1(a) and fig. 1(b). To do the supercell calculations, a *k*-mesh of size 4×2×1 is used.

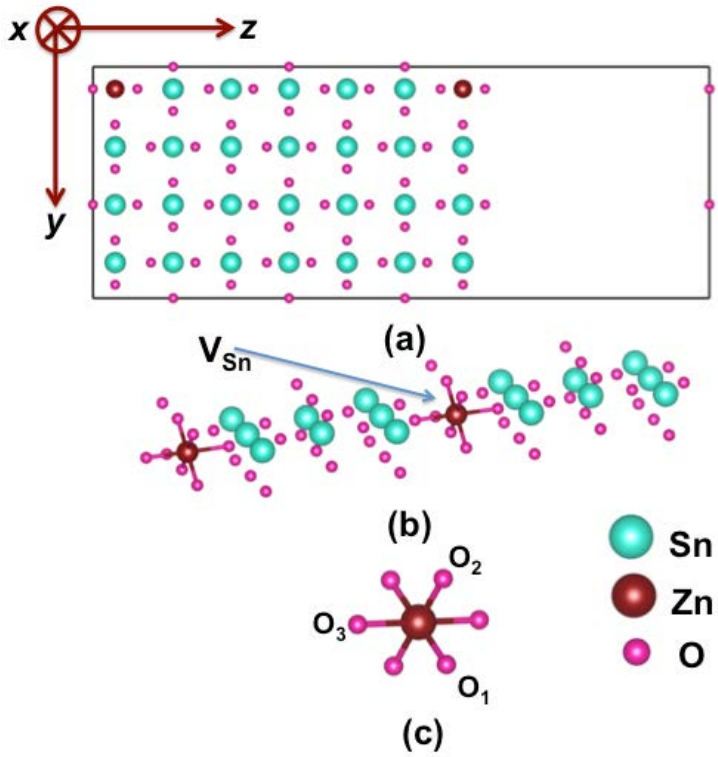

Fig. 1: (a) Schematic picture of the (110) slab with Zn_{Sn}+V_{Sn} defect: (a) and (b) are the sideviews of the slab showing Sn atom substituted by Zn and Sn vacancy; (c) shows the O atoms surrounding the Zn atom in the doped region.

The formation energies of the defects are calculated using the equation:

$$E = E_{def} - E_{undef} + \sum_i \Delta n_i \mu_i$$

where E_{def} and E_{undef} represents the calculated total energies of systems in the presence and absence of defects, respectively. The quantity Δn_i is the difference in the number of atoms of i^{th} species between defect-free and defected supercells and μ_i is the chemical potential of i^{th} species. The chemical potentials of Sn and O atoms are calculated using the cohesive energies of bulk Sn and O_2 molecule respectively. Using these chemical potentials, the formation energies are calculated in Sn-rich and O-rich conditions. Detailed explanation on how to calculate the formation energies in Sn-rich and O-rich conditions is given in Ref.[48].

3. RESULTS AND DISCUSSION

3.1. Vacancies in bulk and at surfaces of SnO_2

Table 1 shows the calculated defect formation energies and magnetic moments per supercell in the presence of intrinsic defects such as V_{Sn} and V_O in bulk and surfaces of SnO_2 in both Sn- and O-rich conditions. Although, there is a large magnetic moment due to V_{Sn} in bulk, the FE for this vacancy is found to be very large~11.5 eV. These data agree very well with previous calculations [5, 49]. FE for V_O is much smaller than that of V_{Sn} but it does not induce any magnetism. We find that doubly ionized oxygen vacancies are also nonmagnetic. However, singly ionized oxygen vacancies do induce magnetism in SnO_2 in agreement with the previous work [4, 36, 38, 50].

Both the (001) and (110) surfaces are also found to show nonmagnetic behaviour in the presence of (neutral and doubly ionized) oxygen vacancies similar to that in bulk SnO_2 which is in agreement with the previous DFT results [15]. The singly ionized V_O on the other hand are

found to be magnetic on (001) surface and nonmagnetic on (110) surface. As expected, FEs of theses defects on surfaces are lower than those in bulk. However, Sn vacancies are still much more diffficult to create even on surfaces and cannot be created instantaneously in any environment. Oxygen vacancies on the other hand can be created instantaneously on surfaces in Sn-rich environment. Overall, creating both types of vacancies on (001) surface are easier than creating them on (110) surface, this is due to the higher surface energy of (001) than that of (110) surface.

The Sn and oxygen vacancies on the symmetric and asymmetric surfaces of (110) are found to have nearly same formation energies. However, Sn vacancy on the symmetric (001) slab has a higher FE of 9.01 eV than on the asymmetric (001) slab which is about 7.5 eV. We also find that the magnetic moments in both the cases are very different. The magnetic moment on the symmetric slab comes out to be zero whereas it is nonzero on the asymmetric slab. This suggests that the magnetic moment of V_{Sn} on (001) surface is perpendicular to the plane of the surface and the magnetic moments from the top and bottom of the surface cancel each other resulting in zero magnetic moment. On asymmetric slab, no such cancellation occurs and the magnetic moment of Sn vacancy on A-(001) surface is almost same as that on S & A-(110) surfaces. This suggests that the magnetic moment of Sn vacancy does not get affected by its environment and surface structure.

Table 1: Defect formation energies (in eV) of O and Sn vacancies in bulk and on surfaces within Sn- and O-rich conditions. M_{cell} is the magnetization of the supercell in μ_B per cell

System	Defect	Sn-rich	O-rich	M_{cell}
Bulk	V_O^0	1.08	3.27	0.00
	V_{sn}^0	11.47	7.08	3.98
S-(001)	V_O^0	-1.68	0.51	0.00
	V_{sn}^0	9.01	4.62	0.00
A-(001)	V_O^0	-1.67	0.52	-0.20
	V_{sn}^0	7.46	3.07	4.18
S-(110)	V_O^0	-0.64	1.56	0.00

	V_{sn}^{0}	10.10	5.71	4.00
A-(110)	V_O^{0}	-0.72	1.48	0.00
	V_{sn}^{0}	10.09	5.71	3.83

On (110) surface, the magnetic moment of V_{Sn} is same for symmetric and asymmetric surfaces suggesting that magnetic moment is in the plane of the surface. From this data, we can say that easy axis of magnetization of V_{Sn} on (001) is perpendicular to surface, whereas it is in-plane for the (110) surface. As mentioned earlier, V_{Sn} are difficult to create as compared to V_O but V_{Sn} are responsible for induced magnetism in SnO_2. Therefore, to induce the magnetism in SnO_2, the FE of V_{Sn} needs to be reduced. One of the ways of doing this would be to introduce the dopants in the system, which is discussed in the next section.

3.2. Effect of Zn doping on intrinsic defects

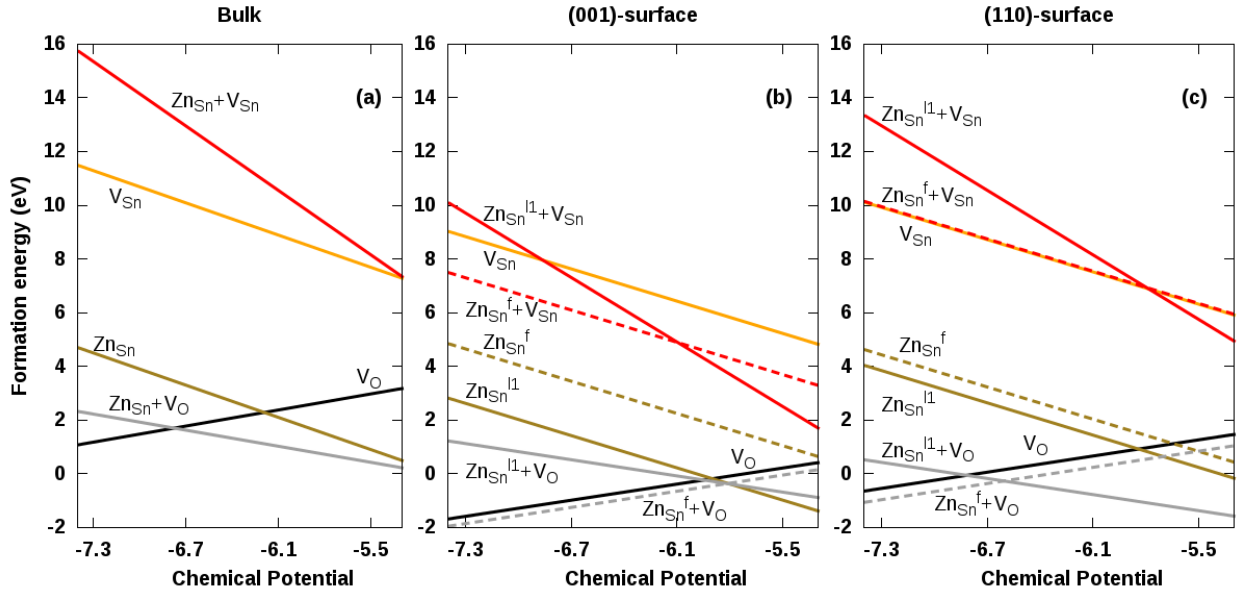

Fig. 2: Formation energies of various isolated defects and defect clusters calculated as a function of oxygen chemical potential: (a) in bulk SnO_2; (b) on (001) surface and (c) on (110) surface. The dashed lines are for doping Zn atom in the bulk region (Zn_{Sn}^{f}) and creating intrinsic defect in the surface layer

Here, we investigate the defect clusters involving Zn and intrinsic defects on the surfaces and their influence on the magnetism in SnO_2. We consider two types of defect clusters: (i) defect

clusters entirely in the surface layer, and (ii) Zn_{Sn} in bulk and the intrinsic defect in the surface layer. Fig. 2 shows the variation in FE of different types of defects in bulk and on surfaces as a function of chemical potential of oxygen [48, 51]. From Fig. 2 (a), the FE of Zn_{Sn} + V_O defect in bulk SnO_2 is 2.31 eV, which is much lower than that of the isolated Zn_{Sn} defect. It is also lower than the FE of isolated oxygen vacancy in O-rich conditions. The further decrease in FE of Zn_{Sn} + V_O is due to the charge compensation between the low valence Zn atoms and negatively charged O atoms. As a result of this charge compensation, the oxygen vacancy associated with the Zn defect quenches the magnetic moment induced by Zn, resulting in zero total magnetization of the cell. FE of Zn_{Sn} + V_{Sn} is 15.7 eV, which is much greater than those of isolated Zn_{Sn} and V_{Sn} defects. However, V_{Sn} with Zn defect increases the magnetic moment by about 40% as compared to the Zn_{Sn} defect alone. On the surfaces, the FE for the Zn_{Sn}+V_O defect cluster further decreases and is lower than those of isolated Zn_{Sn} defects. Interestingly, the Zn_{Sn} + V_O has the lowest FE on (110) surface than in bulk and (001) surface; whereas, all the other isolated defects are easier to form on (001) surface than on (110) surface. The lowest FE for Zn_{Sn} + V_O on (110) surface can be inferred from the charge compensation caused by the reduction in surface co-ordination.

Doping Zn atom in the bulk region of the slab with O vacancy in the surface layer results in the decrease in FE of V_O from 0.51 to 0.25 eV in O-rich conditions on (001) surface. On (110) surface, it decreases from 1.48 to 1.14 eV. On the other hand, Zn_{Sn} defect in the bulk region of the slab does not affect the formation energy of V_{Sn} on (110) surface. However, FE of V_{Sn} decreases from 4.62 to 3.09 eV when Zn atom is substituted for Sn in the bulk region of (001) surfaces. Hence, we find that Zn_{Sn} + V_O is much easier to create than Zn_{Sn} + V_{Sn}, both in bulk and on surfaces and Zn_{Sn} + V_O has the lowest FE of all the intrinsic defects and defect clusters. Unlike the bulk case, this defect cluster is found to induce a finite magnetic moment on (001) surface due to lack of charge compensation caused by reduction in the surface co-ordination. FE of Zn_{Sn}+ V_{Sn} in bulk is much higher than those of isolated Zn_{Sn} and V_{Sn} defects. However, it's FE on (001) surface greatly decreases to 10 eV on (001) surface whereas on (110) surface, it is 13.3 eV and induces a large magnetic moment of ~6.00 μ_B per cell on (110) surface, indicating a ferromagnetic coupling between the two defects. The Zn_{Sn} +V_{Sn} defect is found to have a large increase in the magnetic moment than Zn_{Sn} alone on the (110) surface. The (001) surface does retains the magnetic moment for Zn_{Sn} +V_{Sn} defect cluster, but with antiferromagnetic coupling.

To get the atomic insight of the large magnetism in Zn doped (110) SnO_2 with intrinsic cation defects (V_{Sn}), we plot the orbital projected density of states (DOS) of O atoms surrounding the Zn dopant shown in Fig. 3. We considered only those O atomic sites, which are surrounding the dopant in the supercell. Note that, there are six O atoms surrounding the Zn atom, making a distorted octahedron. Due to the identical environment of three O atoms with other O atoms in the octahedron, we plotted the DOS of those O atoms that have different environment and are shown in Fig. 3(a-c). From the Fig. 3(a-c), it is clear that the magnetism is mainly caused by the 2*p* orbitals of O atoms. The O atoms facing the surface are found to produce higher DOS as compared to others as shown in Fig. 3(b). The large magnetism in the case of Zn_{Sn} +V_{Sn} defect originates from the ferromagnetic coupling of Zn_{Sn} and V_{Sn} defect and the hybridization of nearest neighbor 2*p* orbitals of oxygen atoms with the 3*d* orbitals of Zn dopant. In other words, when the higher valence atom such as Sn is substituted with lower valence dopant Zn, then it impinges holes into the 2*p* orbitals of the neighboring O atoms which leads to shift in the minority DOS of O atoms as shown in Fig. 3(a-c). Note that the dopant itself does not get magnetized extensively (Fig. 3(d)), but induces the magnetism in the neighboring O atoms. The partial DOS of nearest neighbor Sn atoms are not shown because they do not show any appreciable signatures of magnetism.

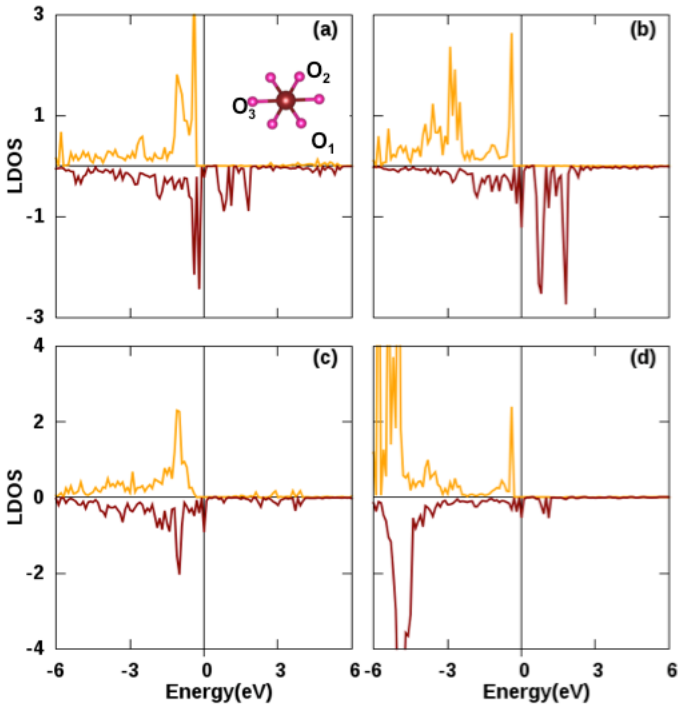

Fig. 2: Spin polarized projected density of states of (a-c) 2*p* orbitals of three types of O (O_1, O_2 and O_3 as shown in the inset) atoms surrounding Zn (d) *d* orbitals of Zn dopant in a $Zn_{Sn}+V_{Sn}$ defect in (110) symmetric slab of SnO_2

4. CONCLUSIONS

In summary, magnetic behavior and energetics of different kinds of defects are studied in bulk, on (001) and (110) surfaces, to understand the role of surfaces in inducing the magnetism in SnO_2 nanoparticles. We find that isolated V_{Sn} gives large magnetic moment, both in bulk and on surfaces, but they are very difficult to create due to large formation energy. However, isolated Zn_{Sn} defects alone are found to have a larger magnetic moment and are also easier to create on both the (001) and (110) surfaces than in bulk. Sn vacancies along with Zn_{Sn} defects ($Zn_{Sn}+V_{Sn}$ defect cluster) become even harder to create even on surfaces (as expected), but they induce a large magnetic moment of 6 μ_B/cell on (110) surface and a small magnetic moment of 2 μ_B/cell on (001) surface. The Zn_{Sn} defects along with O defects are found to have the lowest formation energy of all the defects and induce small magnetism on surfaces. The magnetic moment induced by $Zn_{Sn}+V_O$ defects on (001) surface is larger than (110) surface, however, the FE of this defect is higher on (001) surface than on (110) surface. In fact, $Zn_{Sn}+V_O$ is the only defect that has lower formation energy on (110) surface than on (001) surface. Based on these observations we believe that $Zn_{Sn}+V_O$ defect clusters play an important role on surfaces in inducing the magnetism in SnO_2 nanoparticles.

ACKNOWLEDGMENT

We gratefully acknowledge the financial support from the Research Corporation's Cottrell College Science award and NSF CAREER award (DMR-1255584). Calculations were performed at the HPC center of Idaho National Laboratory.

Refereces

[1] S. A. Wolf *et al., Spintronics: A spin-based electronics vision for the future.* Science, 94 (5546), 1488-1495 (2001).

[2] K. S. Burch, D. D. Awschalom and D. N. Basov, Optical properties of III-Mn-V ferromagnetic semiconductors, J. Magn. Magn. Mater. 320 (23), 3207-3228 (2008).

[3] Sato *et al.*, First-principles theory of dilute magnetic semiconductors, Rev. Mod. Phys. 82, 1633-1690 (2010).

[4] G. Rahman, V. M. García-Suárez and J. M. Morbec, Intrinsic magnetism in nanosheets of SnO_2: A first-principles study, J. Magn. Magn. Mater. 328, 104-108 (2013).

[5] G. Rahman, V. M. García-Suárez, and S. C. Hong, Vacancy-induced magnetism in SnO_2: A density functional study, Phys. Rev. B 78, 184404-1-5 (2008).

[6] A. Punnoose, K. Dodge, J. J. Beltrán, K. M. Reddy, N. Franco, J. Chess, J. Eixenberger and C. A. Barrero, Dopant spin states and magnetism of $Sn_{1-x}Fe_xO_2$ nanoparticles, J. Appl. Phys. 115, 17B34-1-3 (2014).

[7] S. Zhou, K. Potzger, J. Borany, R. Grötzschel, W. Skorupa, M. Helm and J. Fassbender, Crystallographically oriented Co and Ni nanocrystals inside ZnO formed by ion implantation and postannealing, Phys. Rev. B 77, 035209-1-12 (2008).

[8] H. Yanga, R. Hana, Y. Yana, X. Dua, Q. Zhanb, H. Jina, First-principles study of ferromagnetism in Zn- and Cd-doped SnO_2, J. Magn. Magn. Mater. 324, 1764-1769 (2012).

[9] T. C. Kaspar, T. Droubay, S. M. Heald, M. H. Engelhard, P. Nachimuthu, and S. A. Chambers, Hidden ferromagnetic secondary phases in cobalt-doped ZnO epitaxial thin films, Phys. Rev. B 77, 201303-201306(R) (2008).

[10] L. M. Huang, A. L. Rosa, and R. Ahuja, Ferromagnetism in Cu-doped ZnO from first-principles theory, Phys. Rev. B 74, 075206-1-6 (2006).

[11] H. Pan, J. B. Yi, L. Shen, R. Q. Wu, J. H. Yang, J. Y. Lin, Y. P. Feng, J. Ding, L. H. Van, and J. H. Yin, Room-Temperature Ferromagnetism in Carbon-Doped ZnO, Phys. Rev. Lett. 99, 127201-1-4 (2007).

[12] Q. J. Wang, J. B. Wang, X. L. Zhong, Q. H. Tan, Z. Hu and Y. C. Zhou, Magnetism mechanism in ZnO and ZnO doped with nonmagnetic elements X (X = Li, Mg, and Al): A first-principles study, Appl. Phys. Lett. 100, 132407-1-5 (2012).

[13] A. Fakhim Lamrani, M. Belaiche, A. Benyoussef, A. El Kenz, E. H. Saidi, Ferromagnetism in Mo-doped TiO2 Rutile from Ab Initio Study, J. Super. Nov. Magn. 25, 503-507 (2012).

[14] S. K. Srivastava, P. Lejay, A. Hadj-Azzem, G. Bouzerar, Non-magnetic impurity induced magnetism in Li-Doped SnO_2 nanoparticles, J. Superc. Nov. Mag. 27, 487-492 (2014).

[15] G. Rahman, V. M. García-Suárez, Surface-induced magnetism in C-doped SnO_2, Appl. Phys. Lett. 96, 052508-1-3 (2010).

[16] W. –Z. Xiao, L. –L. Wang, L. Xu, Q. Wan, B. S. Zou, Magnetic properties in nitrogen-doped SnO_2 from first-principle study, Sol. Stat. Comm. 149, 1304-1307 (2009).

[17] L. –B. Shi, G. –Q. Qi and H. –K. Dong, First-principles study of the magnetic properties of Zn-doped SnO_2, Mat. Sci. Sem. Proc. 16, 877-883 (2013).

[18] W. Wei, Y. Dai, M. Guo, K. Lai and B. Huang, Density functional study of magnetic properties in Zn-doped SnO_2, J. Appl. Phys. 108, 093901-1-5 (2010).

[19] Y. –L. Zhang, X. –M. Tao and M. –Q. Tan, Origin of ferromagnetism in Zn-doped SnO_2 from first-principles study, J. Magn. Magn. Mater. 325, 7-12 (2013).

[20] K. –C. Zhang, Y. –F. Li, Y. Liu and Y. Zhu, Ferromagnetism of Cd doped SnO_2: A first-principles study, J. Appl. Phys. 112, 043705-1-4 (2012).

[21] W. Wei, Y. Dai, B. Huang, Role of Cu doping in SnO2 sensing properties towards H_2S, J. Phys. Chem. C 115, 18597-18602 (2011).

[22] M. Batzill and U. Diebold, The surface and material science of tin oxide, Prog. Surf. Sci. 79, 47-154 (2005).

[23] J. Hays, A. Punnoose, R. Baldner, M. H. Engelhard, J. Peloquin, and K. M. Reddy, Relationship between the structural and magnetic properties of Co-doped SnO_2 nanoparticles, Phys. Rev. B 72, 075203-1-7 (2005).

[24] H. Wang and A. L. Rogach, Hierarchical SnO_2 nanostructures: Recent advances in design, synthesis, and applications, Chem. Mater. 26, 123-133 (2014).

[25] K. Ueda, H. Tabata and T. Kawa, Magnetic and electric properties of transition-metal-doped ZnO films, Appl. Phys. Lett. 79, 988-990 (2001).

[26] Ogale *et al.* High temperature ferromagnetism with a giant magnetic moment in transparent Co-doped $SnO_{2-\delta}$, Phys. Rev. Lett. 91, 077205-1-4 (2003).

[27] A. F. Hebard, R. P. Rairigh, J. G. Kelly, S. J. Pearton, C. R. Abernathy, S. N. G. Chu and R. G. Wilson, Mining for high Tc ferromagnetism in ion-implanted dilute magnetic semiconductors, J. Phys. D: Appl. Phys. 37, 511-517 (2004).

[28] J. M. D. Coey, A. P. Douvalis, C. B. Fitzgerald, and M. Venkatesan, Ferromagnetism in Fe-doped SnO_2 thin films. Appl. Phys. Lett. 84(8), 1332-1334 (2004).

[29] N. H. Hong and J. Sakai, Ferromagnetic V-doped SnO_2 thin films. Phys. B: Cond. Matt. 358(1-4), p. 265-268 (2005).

[30] N. H. Hong, J. Sakai, W. Prellier and A. Hassini, Transparent Cr-doped SnO_2 thin films: ferromagnetism beyond room temperature with a giant magnetic moment, J. Phys.: Cond. Matt. 17(10), 1697-1702 (2005).

[31] C. B. Fitzgerald *et al.*, Magnetism in dilute magnetic oxide thin films based on SnO_2, Phys. Rev. B 74, 115307-1-10 (2006).

[32] T. Dietl, a ten-year perspective on dilute magnetic semiconductors and oxides. Nat. Mater. 9, 965-974 (2010).

[33] H. Yanga, R. Hana, Y. Yana, X. Dua, Q. Zhanb and H. Jina, First-principles study of ferromagnetism in Zn- and Cd-doped SnO_2, J. Mag. Magn. Mater. 324, 1764-1769 (2012).

[34] X. Liu, J. Iqbal, Z. Wu, B. He and R. Yu, Structure and room-temperature ferromagnetism of Zn-doped SnO_2 nanorods prepared by solvothermal method, J. Phys. Chem. C 114, 4790-4796 (2010).

[35] W. –Z. Xiao, L. –l. Wang, B. Meng and G. Xiao, First-principles insight into the surface magnetism of Cu-doped SnO_2 (110) thin film, RSC Adv. 4, 39860-39865 (2014)

[36] P. Raghani and B. Ramanujam, Magnetism of Zn-doped SnO_2: Role of surfaces, J. Appl. Phys. 115, 17C114-1-3 (2014).

[37] G. S. Chang *et al.* Oxygen-vacancy-induced ferromagnetism in undoped SnO_2 thin films, Phys. Rev. B 85, 165319-1-5 (2012).

[38] H. Wang, Y. Yan, K. Li, X. Du, Z. Lan, and H. Jin, Role of intrinsic defects in ferromagnetism of SnO_2: First-principles calculations, Phys. Stat. Sol.(b) 247, 444-448 (2010).

[39] A. P. Guimarães, Principles of nanomagnetism, Springer-Verlag, Berlin, Heidelberg (2009).

[40] J. M. D. Coey, Magnetism and magnetic materials, Cambridge University Press (2009).

[41] Kumar *et al.*, Permanent magnetism of intermetallic compounds between light and heavy transition-metal elements, J. Phys.: Cond. Matt. 26, 064209-1-8 (2014).

[42] J. Oviedo, M.J Gillan, Energetics and structure of stoichiometric SnO_2 surfaces studied by first-principles calculations, Surf. Sci. 463, 93-101 (2000).

[43] W. Bergermayer and I. Tanaka, Reduced SnO_2 surfaces by first-principles calculations, Appl. Phys. Lett. 84, 909-911 (2004).

[44] P. Giannozzi, QUANTUMESPRESSO: a modular and open-source software project for quantum simulations of materials, J. Phys.: Cond. Matt. 21, 395502-1-19 (2009).

[45] J. P. Perdew, K. Burke, and M. Ernzerhof, Generalized gradient approximation made simple, Phys. Rev. Lett. 77, 3865–3868 (1996).

[46] J. Haines and J. M. Léger, X-ray diffraction study of the phase transitions and structural evolution of tin dioxide at high pressure: Relationships between structure types and implications for other rutile-type dioxides, Phys. Rev. B 55, 11144-11154 (1997).

[47] H. J. Monkhorst and J. D. Pack, Special points for Brillouin zone integrations, Phys. Rev. B 13, 5188-5192 (1976).

[48] P. Raghani, D. Daniel and D. P. Butt, Electronic properties of Ca doped $LaFeO_3$:A first-principles study, Sol. Stat. Ion. 249-250, 184-190 (2013).

[49] G. Rahman, N. U. Din, V. M. García-Suárez, and E. Kan, Stabilizing intrinsic defects in SnO_2, Phys. Rev. B 87, 205205-1-10 (2013).

[50] A. Espinosa, N. Sánchez, J. Sánchez-Marcos, A. Andrés and M. C. Muñoz, Origin of the magnetism in undoped and Mn-doped SnO_2 thin films: Sn vs oxygen vacancies, J. Phys. Chem. C 115(49), 24054-24060 (2011).

[51] V. Sharma, G. Pilania, G. A. Rossetti, Jr., K. Slenes and R. Ramprasad, Comprehensive examination of dopants and defects in $BaTiO_3$ from first principles, Phys. Rev. B 87, 134109-1-7 (2013).